The Astronomical Journal, 159:179 (10pp), 2020 April https://doi.org/10.3847/1538-3881/ab7899

Potential Themis-family Asteroid Contribution to the Jupiter-family Comet Population

Henry H. Hsieh[1,2], Bojan Novaković[3], Kevin J. Walsh[4], and Norbert Schörghofer[1]
[1] Planetary Science Institute, 1700 East Fort Lowell Rd., Suite 106, Tucson, AZ 85719, USA; hhsieh@psi.edu
[2] Institute of Astronomy and Astrophysics, Academia Sinica, P.O. Box 23-141, Taipei 10617, Taiwan
[3] Department of Astronomy, Faculty of Mathematics, University of Belgrade, Studentski trg 16, 11000 Belgrade, Serbia
[4] Southwest Research Institute, 1050 Walnut St., Suite 400, Boulder, CO 80302, USA
Received 2019 November 13; revised 2020 February 18; accepted 2020 February 19; published 2020 March 30

Abstract

Recent dynamical analyses suggest that some Jupiter family comets (JFCs) may originate in the main asteroid belt instead of the outer solar system. This possibility is particularly interesting given evidence that icy main-belt objects are known to be present in the Themis asteroid family. We report results from dynamical analyses specifically investigating the possibility that icy Themis family members could contribute to the observed population of JFCs. Numerical integrations show that such dynamical evolution is indeed possible via a combination of eccentricity excitation apparently driven by the nearby 2:1 mean-motion resonance with Jupiter, gravitational interactions with planets other than Jupiter, and the Yarkovsky effect. We estimate that, at any given time, there may be tens of objects from the Themis family on JFC-like orbits with the potential to mimic active JFCs from the outer solar system, although not all, or even any, may necessarily be observably active. We find that dynamically evolved Themis family objects on JFC-like orbits have semimajor axes between 3.15 and 3.40 au for the vast majority of their time on such orbits, consistent with the strong role that the 2:1 mean-motion resonance with Jupiter likely plays in their dynamical evolution. We conclude that a contribution from the Themis family to the active JFC population is plausible, although further work is needed to better characterize this contribution.

Unified Astronomy Thesaurus concepts: Main belt asteroids (2036); Short period comets (1452); Orbits (1184); Orbital evolution (1178)

1. Introduction

1.1. Background

The Themis asteroid family has come to be of particular interest in solar system science in recent years. At least three main-belt comets (MBCs, which exhibit comet-like activity indicative of sublimating ice, yet have asteroid-like orbits; Hsieh & Jewitt 2006), namely 133P, 176P, and 288P, are members of the family (Hsieh et al. 2018). A fourth MBC, 238P, has also been proposed to be a past member of the family (Haghighipour 2009). Water ice frost has also been reported on large Themis family members, (24) Themis and (90) Antiope (Campins et al. 2010; Rivkin & Emery 2010; Hargrove et al. 2015). Since asteroid family members are believed to be compositionally similar (e.g., Masiero et al. 2015), these findings suggest that ice could be widespread within the family.

Interesting dynamical results related to the main asteroid belt have also been reported recently. Fernández & Sosa (2015) found that certain known Jupiter-family comets (JFCs) are significantly more dynamically stable than other JFCs, and proposed that they could originate in the asteroid belt, rather than the outer solar system. Meanwhile, Hsieh & Haghighipour (2016) found dynamical pathways by which synthetic test particles with initially asteroid-like orbits could evolve onto JFC-like orbits, and reached a similar conclusion that the JFC population could contain asteroidal interlopers. However, Fernández & Sosa (2015) did not trace full dynamical pathways from the asteroid belt to their candidate asteroidal JFC interlopers in their study, while Hsieh & Haghighipour (2016) did not use test particles representing real solar system objects for their study.

The Themis family's proximity to the strong 2:1 mean-motion resonance (MMR) with Jupiter (hereafter, "the 2:1 MMR") at 3.278 au makes it likely that objects have been removed from the family over time (e.g., Morbidelli et al. 1995). Additional sources of instability include the 9:4 MMR with Jupiter (hereafter, "the 9:4 MMR") at 3.031 au, which bounds the family on its inner edge, and the 11:5 MMR with Jupiter (hereafter, "the 11:5 MMR") at 3.077 au, which intersects the family. If icy Themis family asteroids are able to reach low-perihelion JFC-like orbits with Tisserand parameter values of $T_J < 3$ (see Kresák 1972) while retaining at least some near-surface ice, they could become active and be observationally and dynamically indistinguishable from JFCs from the outer solar system, at least superficially. To investigate this possibility, we have conducted numerical integrations to investigate the long-term dynamical behavior of Themis family members.

2. Experimental Design

We investigated the Themis family by selecting all 4782 members identified by Nesvorny (2015) and, following the method of Hsieh et al. (2012), generating four dynamical clones per object using σ values of $\sigma_a = 0.001$ au, $\sigma_e = 0.001$, and $\sigma_i = 0.^\circ01$ for their semimajor axes, eccentricities, and inclinations, respectively. These σ values were chosen to be relatively large (e.g., larger than any of the orbital elements' formal uncertainties) in order to characterize the dynamical environment occupied by each Themis family asteroid, help account for chaotic effects, and allow for a rough assessment of the potential effects of collisions that could impart one-time impulses to post-impact bodies. We integrated each original object and its clones (i.e., 5 test particles per object, or 23,910 test particles in total) forward in time for 100 Myr under the gravitational influence of the seven major planets other than Mercury using the hybrid integrator in the `mercury` *N*-body

integration package (Chambers 1999). Nongravitational forces were not included. Integrations were performed using the Planetary Science Institute Computing Center's (PSICC) Torque cluster as well as a 64 vCPU Google Compute Engine virtual machine.[5]

In order to investigate the evolution of our test particles, we recorded each particle's intermediate orbital elements (IOEs) at 1000 yr intervals. To smooth out short-timescale fluctuations, we computed quasi-mean orbital elements by taking running averages of 100 time steps centered on each time step. We then classified these quasi-mean IOEs as within the Themis family (i.e., based on the osculating orbital element bounds of the current family), outside the Themis family but still dynamically similar to main-belt asteroids (MBAs), or dynamically similar to JFCs using the following criteria:

1. Themis-family-like: $3.020\ \mathrm{au} < a_{\mathrm{ioe}} < 3.270\ \mathrm{au}$, $0.070 < e_{\mathrm{ioe}} < 0.225$, and $0.^{\circ}040 < i_{\mathrm{ioe}} < 3.^{\circ}450$
2. Non-Themis-MBA-like: $2.064\ \mathrm{au} < a_{\mathrm{ioe}} < 3.277\ \mathrm{au}$, $T_J > 3.05$, $q_{\mathrm{ioe}} > (Q_{\mathrm{Mars,max}} + 1.5r_{H,\mathrm{Mars}})$, and $Q_{\mathrm{ioe}} < (q_{\mathrm{Jup,min}} - 1.5r_{H,\mathrm{Jup}})$ (following Hsieh & Haghighipour 2016)
3. JFC-like: $2.00 < T_J < 3.00$, $q_{\mathrm{ioe}} < Q_{\mathrm{Jup,min}}$, and $Q_{\mathrm{ioe}} > (q_{\mathrm{Jup,max}} - 1.5r_{H,\mathrm{Jup}})$ (following Tancredi 2014)

where the Hill radii of Mars and Jupiter are $r_{H,\mathrm{Mars}} = 0.007$ au and $r_{H,\mathrm{Jup}} = 0.355$ au, respectively. Mars's maximum aphelion distance over our integration period is $Q_{\mathrm{Mars,max}} = 1.714$ au, Jupiter's minimum and maximum perihelion distances are $q_{\mathrm{Jup,min}} = 4.880$ au and $q_{\mathrm{Jup,max}} = 5.071$ au, respectively, and Jupiter's minimum aphelion distance is $Q_{\mathrm{Jup,min}} = 5.333$ au. All of these values are obtained from our integrations themselves, where for reference Mars's mean aphelion distance is $Q_{\mathrm{Mars,mean}} = 1.666$ au, and Jupiter's mean perihelion and aphelion distances are $q_{\mathrm{Jup,mean}} = 4.951$ au and $Q_{\mathrm{Jup,mean}} = 5.455$ au, respectively, based on planetary orbital elements from JPL.[6] To reduce complexity, we did not compute Minimum Orbit Intersection Distances (MOIDs) as part of classifying orbits as JFC-like as Tancredi (2014) did in order to exclude objects that did not have strong gravitational interactions with Jupiter. We note however that the `mercury` integration software we used indicated that 99.1% of particles with JFC-like IOEs experienced actual close encounters with Jupiter (within $3r_{H,\mathrm{Jup}}$) and thus can safely be assumed to satisfy the fundamental characteristic of having strong interactions with Jupiter underlying the MOID requirement set by Tancredi (2014) for JFC-like objects.

For reference, we also classify IOEs that meet the following dynamical criteria for Centaurs, long period comets (LPCs), and dynamically asteroidal near-Earth objects (NEOs):

1. Centaur-like: $2.00 < T_J$, $q_{\mathrm{ioe}} > Q_{\mathrm{Jup,max}}$, $q_{\mathrm{ioe}} < a_{\mathrm{Ura}}$
2. LPC-like: $T_J < 2.00$
3. NEO-like (dynamically asteroidal): $q_{\mathrm{ioe}} < 1.3$ au, $T_J > 3.05$

where Jupiter's maximum aphelion distance is $Q_{\mathrm{Jup,min}} = 5.525$ au and Uranus's mean semimajor axis distance is $a_{\mathrm{Ura}} = 19.201$ au. Since the primary motivation of this work is to specifically investigate connections between the Themis family and JFCs, however, we will not discuss these types of IOEs in detail in this work.

To gain a sense of the potential impacts of nongravitational perturbations on the dynamical evolution of Themis family asteroids as well as perform an independent check of our initial integrations, we also ran two small-scale sets of follow-up integrations including the Yarkovsky effect using the Orbit9 integrator (Milani & Nobili 1988) in the OrbFit package.[7] In the first set of follow-up integrations, we integrated all 4782 cataloged Themis family asteroids under the gravitational influence of the Sun and the four major outer planets and the Yarkovsky effect, but to reduce computational time, did not include the terrestrial planets. For these integrations, object sizes were determined using cataloged absolute magnitudes and assumed geometric albedos of $p = 0.07$. A reference maximum drift rate of $(da/dt)_{\mathrm{max,1km}} = 6 \times 10^{-4}$ au Myr^{-1} for a body with a diameter of $D = 1$ km was adopted from Spoto et al. (2015) and scaled for each object's size using $(da/dt)_{\mathrm{max}} = (da/dt)_{\mathrm{max,1km}}/D$ as the maximum drift rate for objects with diameters of D in kilometers (see Bottke et al. 2006).

Assuming an isotropic distribution of spin axis orientations, a random value of da/dt between $-(da/dt)_{\mathrm{max}}$ and $(da/dt)_{\mathrm{max}}$ was then assigned to each body. Our second set of follow-up integrations included the gravitational influence of the Sun and seven major planets (i.e., including the terrestrial planets except for Mercury) and the Yarkovsky effect, but only included 500 test particles (~10% of the total Themis family population). Both sets of integrations were run for 100 Myr, i.e., the same duration as our initial integrations. A detailed analysis of these and other integrations to investigate the impacts of nongravitational effects on Themis family asteroid evolution will be presented in a future paper. Hereafter, unless otherwise specified, our analysis and discussion will focus on our purely gravitational integrations.

3. Results and Analysis

3.1. Overview

The results of our primary integrations are summarized in Table 1. We find that the vast majority of Themis family asteroids and their dynamical clones are dynamically stable and remain within the family over our entire 100 Myr integration period, as expected for members of a large low-inclination, moderate-eccentricity asteroid family in the main asteroid belt. We do however find that 58 real Themis family members (1.2% of the family) and dynamical clones of an additional 843 family members (17.6% of the family) had IOEs outside the Themis family but still within the asteroid belt for the entire integration period. Meanwhile, 32 real Themis family members (0.7% of the family) and dynamical clones of an additional 335 family members (7.0% of the family) were ejected from the solar system ($a > 100$ au) within the integration period. Virtually all of these unstable test particles had JFC-like IOEs, where a small number of these particles also reached Centaur-like, LPC-like, or dynamically asteroidal NEO-like IOEs.

In Figures 1 and 2, we show an example of the dynamical evolution undergone by a test particle representing current Themis family member (12,360) Unilandes that was found to evolve from a Themis-family-like orbit to a JFC-like orbit

[5] https://cloud.google.com/compute/
[6] https://ssd.jpl.nasa.gov/?planet_pos
[7] http://adams.dm.unipi.it/orbfit/

Table 1
Integration Results Summary (No Yarkovsky Effect)

	Entire Themis family[a]				2:1 MMR region[b]			
	$n_{\rm real}$[c]	$f_{\rm real}$[d]	$n_{\rm all}$[e]	$f_{\rm all}$[f]	$n_{\rm real}$[c]	$f_{\rm real}$[d]	$n_{\rm all}$[e]	$f_{\rm all}$[f]
Dynamically stable	4750	0.9933	4415	0.9233	680	0.9605	421	0.5946
Themis only[g]	4692	0.9812	3514	0.7348	678	0.9576	351	0.4958
Main-belt, non-Themis[h]	58	0.0121	901	0.1884	2	0.0028	70	0.0989
Dynamically unstable	32	0.0067	367	0.0767	28	0.0395	287	0.4054
JFC-like[i]	32	0.0067	365	0.0767	28	0.0395	287	0.4054
Centaur-like[j]	8	0.0017	129	0.0270	6	0.0085	86	0.1215
NEO-like ($T_J > 3.05$)[k]	3	0.0006	25	0.0052	1	0.0014	11	0.0155
LPC-like[l]	2	0.0004	72	0.0151	2	0.0028	67	0.0946
Total	4782	1.0000	4782	1.0000	708	1.0000	708	1.0000

Notes.
[a] Results for all 4782 Themis family members.
[b] Results for Themis family members with osculating elements within the region of influence of the 2:1 MMR described in the text.
[c] Number of test particles representing real Themis family members in specified category.
[d] Fraction of test particles representing real Themis family members in specified category.
[e] Number of Themis family members with one or more test particles representing dynamical clones in specified category.
[f] Fraction of Themis family asteroids with one or more test particles representing dynamical clones in specified category.
[g] Test particles that remain within the Themis family for the entire integration period.
[h] Test particles that evolve beyond the Themis family but have MBA-like IOEs for the entire integration period.
[i] Test particles with JFC-like IOEs.
[j] Test particles with Centaur-like IOEs.
[k] Test particles with $T_J > 3$ NEO-like IOEs.
[l] Test particles with LPC-like IOEs.

during our integrations. As with many of the clones found to reach JFC-like orbits (as defined in Section 2) in our integrations, this particle starts out in the region affected by the 2:1 MMR with Jupiter (see Figure 1). The resonance then causes eccentricity and inclination excitation (Figures 2(b) and (c)), eventually driving the particle to Mars- and Jupiter-crossing orbits (Figures 2(d) and (e)) and comet-like T_J values (Figure 2(f)) as its increasing eccentricity causes it to interact more strongly with the major planets (Figure 2(g)).

Semimajor axis versus eccentricity and inclination plots (Figure 3) indicate that the vast majority of real Themis family asteroids with IOEs outside the Themis family but still within the asteroid belt largely originate near the 11:5 MMR. Meanwhile, although a few test particles with JFC-like IOEs also originate near the 11:5 MMR, the vast majority start near the 2:1 MMR. We mark the boundary of the region affected by the 2:1 MMR in Figure 3(c). This boundary is visually approximated from the extent in semimajor axis-eccentricity space of the starting orbital elements of test particles found to eventually evolve onto JFC-like orbits, and is given by $e = -2.5a + 8.15$ (for a in au). We use an empirically approximated boundary for the 2:1 MMR's region of influence rather than a theoretically derived resonance boundary (e.g., Murray & Dermott 2000; Wang & Malhotra 2017), because the former is simpler to implement and the potentially greater accuracy of the latter is not necessary for our purposes in this work.

For reference, there are 708 known Themis family members (Table 1) and ~13,000 total MBAs in the near-MMR region of interest that we have identified. Of those 708 known Themis family members (~15% of the family), 28 real family members (4.0% of this subset of the family) and dynamical clones of an additional 259 family members (36.6% of this subset of the family) reach JFC-like IOEs during our integrations.

In our first set of follow-up integrations including the Yarkovsky effect, we find that even more test particles reach JFC-like orbits than in our purely gravitational integrations. Specifically, we find that 73 Themis family asteroids, 67 of which are located in the region of influence of the 2:1 MMR discussed above, reach JFC-like IOEs, representing roughly a factor of two increase over the number of Themis family asteroids with JFC-like IOEs in our original integrations. In our second set of follow-up integrations (including the Yarkovsky effect and all seven major planets besides Mercury as perturbers), we find that 8 out of 500 particles reach JFC-like IOEs, representing an additional ~5%–10% increase over the number of particles with JFC-like IOEs from our first set of follow-up integrations.

3.2. Analysis of JFC-like Particles

We seek to better assess whether icy objects originating in the Themis family could plausibly be mistaken for JFCs from the outer solar system, and, if so, how they might potentially be identified. To do so, we examine the distribution in orbital element space of the JFC-like IOEs attained by particles in our integrations and compare it to those of objects in the present-day known JFC population.

One immediately apparent feature of the JFC-like IOEs from our integrations is that 88.8% have semimajor axes within 0.125 au of the 2:1 MMR (i.e., between 3.15 and 3.40 au), likely reflecting the strong role that this resonance plays in driving these particles onto JFC-like orbits. Focusing on this particular region, we compare the semimajor axis, eccentricity, inclination, longitude of the ascending node, argument of perihelion, and T_J distributions of the 790,765 IOEs of test particles representing both real Themis family asteroids and their clones with semimajor axes between 3.0 au and 3.5 au

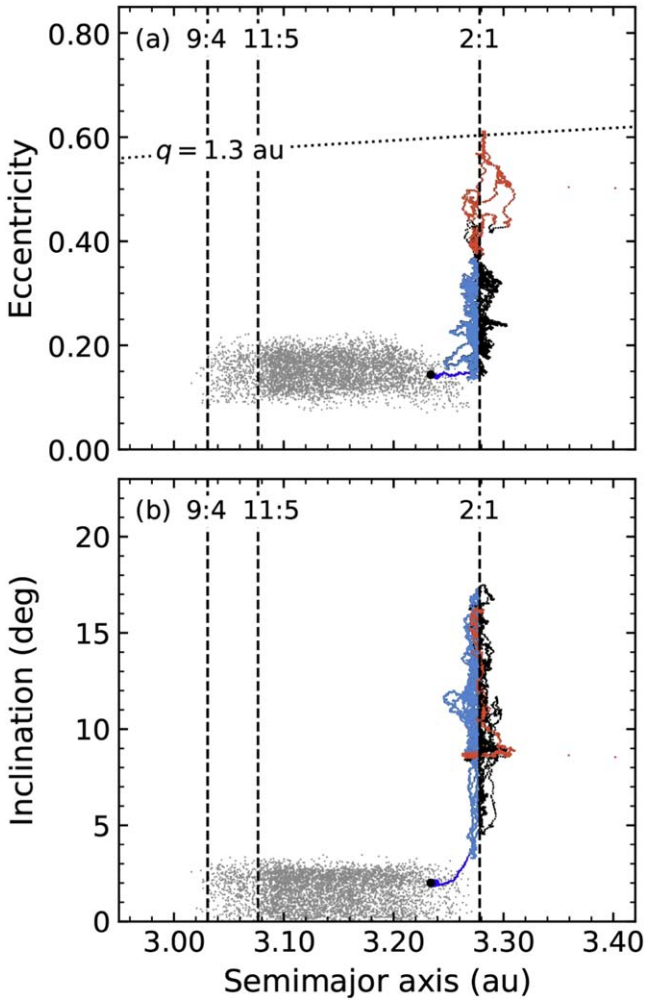

Figure 1. Plots of the forward dynamical evolution of a test particle representing Themis family member (12360) Unilandes in (a) semimajor axis vs. eccentricity space, and (b) semimajor axis vs. inclination space, where large black circles mark the starting orbital elements of the asteroid, small gray dots mark the orbital elements of current Themis family members, small dark blue dots mark IOEs for the asteroid that lie within the osculating orbital element boundaries of current Themis family members, small light blue dots mark IOEs for the asteroid that meet the criteria for main-belt-like orbits described in the text, and small red dots mark IOEs for the asteroid to meet the criteria for JFC-like orbits described in the text. Vertical dashed lines mark the 9:4, 11:5, and 2:1 mean-motion resonances with Jupiter, as labeled.

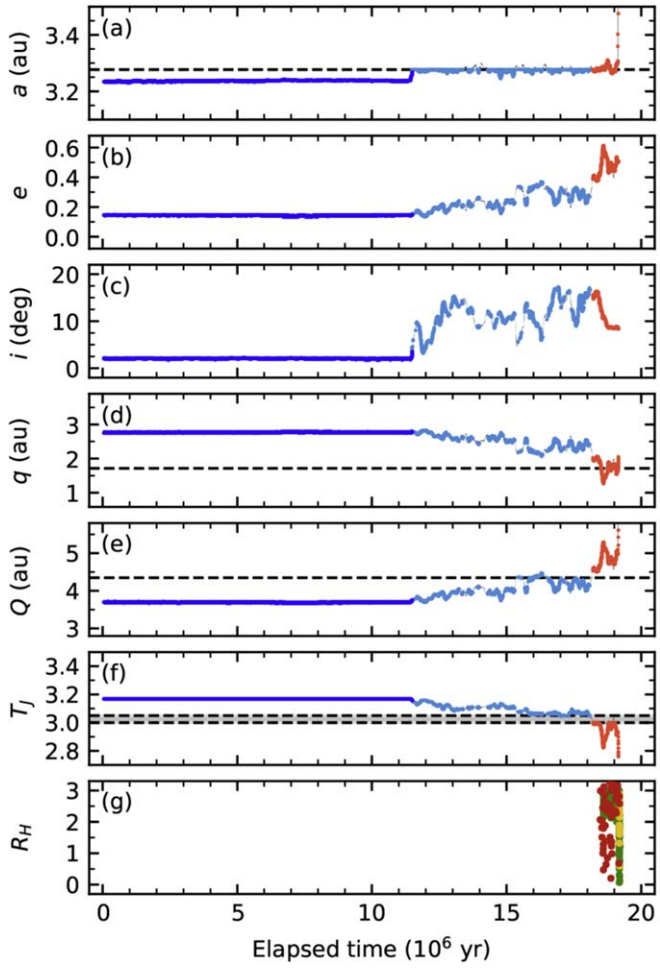

Figure 2. Plots of the forward dynamical evolution of a test particle representing Themis family member (12360) Unilandes, specifically (a) semimajor axis (b) eccentricity, (c) inclination, (d) perihelion, (e) aphelion, and (f) T_J vs. time, and (g) plots of distances of close encounters with Mars, Saturn, and Jupiter in terms of Hill radii (R_H) of each planet as a function of time. In panels (a)–(d), small dark blue dots mark IOEs for the asteroid that lie within the osculating orbital element boundaries of current Themis family members, small light blue dots mark IOEs for the asteroid that meet the criteria for main-belt-like orbits described in the text, and small red dots mark IOEs for the asteroid to meet the criteria for JFC-like orbits described in the text. Horizontal dashed lines in panels (a), (d), and (e) mark the heliocentric distances of the 2:1 MMR, $Q_{\mathrm{Mars,max}}$, and $q_{\mathrm{Jup,min}}$, respectively. Horizontal dashed lines and the gray shaded region in panel (f) mark the approximate T_J boundary region between dynamically asteroidal and dynamically cometary orbits. In panel (g), red dots mark close encounters with Mars, green dots mark close encounters with Jupiter, and yellow dots mark close encounters with Saturn.

with the 89 real JFCs cataloged by JPL[8] as of 2019 October 1 found within the same semimajor axis range (Figure 4).

The semimajor axis distribution of the sample of real JFCs plotted in Figure 4 shows that there are actually relatively few JFCs in the semimajor axis range within which the majority of the JFC-like IOEs of our test particles are found, suggesting that if dynamically evolved Themis family asteroids are indeed present among active JFCs, they may only comprise a small subset of the population. As such, close matches of the orbital element distributions of the JFC-like IOEs of our test particles and the real JFC population are not necessarily expected or required to validate our results, as long as they are not fundamentally incompatible with each other. The distributions of the longitudes of the ascending node and arguments of perihelion for our JFC-like test particles do differ somewhat from those of real JFCs with 3.0 au $< a <$ 3.5 au, but given the natural circulation of these angles over time and the far smaller sample of real JFCs relative to JFC-like test particle IOEs, we do not regard the differences in these distributions as significant. Meanwhile, while the JFC-like IOEs of our test particles cover a somewhat larger inclination range than those real JFCs, we otherwise find that those IOEs span similar ranges of eccentricities, inclinations, and T_J values as real JFCs within the targeted semimajor axis range and have similar distributions within those ranges, and are therefore generally compatible with the real JFC population.

To estimate the potential contribution of Themis family asteroids to the JFC population based on the integrations presented here, we note that measurements of 89 JFC nuclei (Fernández et al. 2013) found nuclei diameters down to

[8] https://ssd.jpl.nasa.gov/?sb_elem

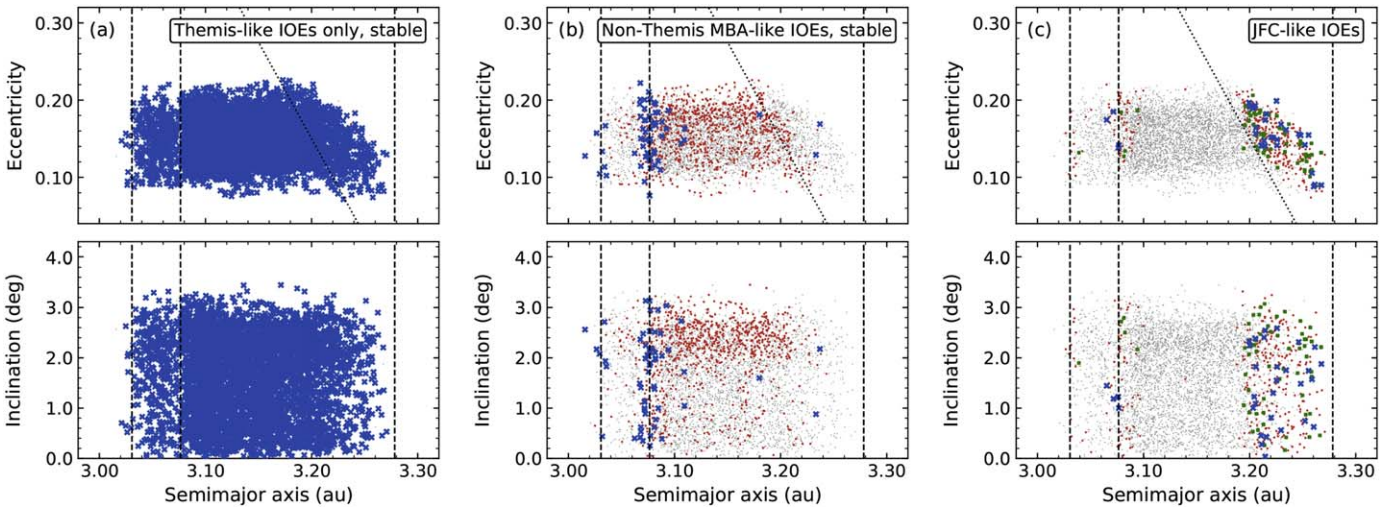

Figure 3. Semimajor axis vs. eccentricity (upper panels) and inclination (lower panels) plots showing the starting osculating orbital elements of test particles that (a) remain within the Themis family for the entire integration period, (b) evolve beyond the Themis family but remain within the main belt for the entire integration period, and (c) reach JFC-like IOEs during the integration period. In all panels, small gray dots mark the orbital elements of all currently known Themis family members, blue X's mark real Themis family asteroids, and small red dots mark dynamical clones, while in panel (c), green squares mark Themis family members found to reach JFC-like IOEs in our first set of follow-up integrations including the Yarkovsky effect. Vertical dashed lines in each panel denote, from left to right, the 9:4, 11:5, and 2:1 mean-motion resonances with Jupiter. Diagonal dotted lines in each panel show the boundary of the empirically identified region of influence of the 2:1 MMR in semimajor axis vs. eccentricity space.

$\sim$1 km. We convert absolute magnitudes (H_V) cataloged by the Minor Planet Center for Themis family asteroids to effective diameters ($D_{\rm eff}$) in kilometers using

$$D_{\rm eff} = \left(\frac{8.96 \times 10^{16}}{p_V} \times 10^{0.4(m_\odot - H_V)} \right)^{0.5} \quad (1)$$

assuming V-band albedos of $p_V = 0.05$ and a V-band solar magnitude of $m_\odot = -26.71$ mag (see Jewitt 1991; Fernández et al. 2000). By fitting a power law to the differential size–frequency distribution of the source population of the JFC-like particles in our integrations and extrapolating to smaller sizes where the known population is likely incomplete, we should be able to use the fraction of particles that reach JFC-like orbits in our integrations and the total length of our integration period to estimate the total flux of objects onto such orbits.

We note, however, that plots of the semimajor axis distributions of Themis family asteroids in different size bins (Figure 5) show that larger asteroids are more concentrated toward the center of the family in semimajor axis space, with a larger fraction of smaller asteroids found farther from the center. This size-dependent semimajor axis distribution is consistent with the previously noted phenomenon of size-dependent Yarkovsky-driven semimajor axis drift in asteroid families (e.g., Vokrouhlický et al. 2006; Bottke et al. 2006; Walsh et al. 2013). To mitigate the effect of this uneven distribution of objects of different sizes on our results, we restrict our analysis on the region of influence of the 2:1 MMR defined in Section 3.1, instead of the full family.

Visually fitting a power law to the differential size–frequency distribution of Themis family asteroids in the region of influence of the 2:1 MMR (Figure 6), we find an approximate slope parameter of -2.8 and an estimated $\sim 5 \times 10^4$ Themis family asteroids with diameters of 1 km in this region. Assuming that the fraction ($\sim$4%; see Table 1) of known Themis family members in the near-MMR region that reach JFC-like orbits over a 100 Myr integration period found in our purely gravitational integrations remains similar for the complete population in this region, we expect on the order of $\sim$2000 Themis family objects from the near-MMR region could evolve onto JFC-like orbits every 100 Myr under the influence of gravity alone. We find a mean residence time on JFC-like orbits of $t \sim 1 \times 10^6$ yr for Themis family objects that reach such orbits during our integrations. Thus, the $\sim$2000 objects per 100 Myr found to reach JFC-like orbits should collectively spend a total of $\sim 2 \times 10^9$ yr on such orbits, suggesting that, on average, we should expect $\sim$20 objects from the Themis family on JFC-like orbits at any given time with the potential to mimic active JFCs from the outer solar system.

There are many uncertainties associated with this analysis, however. First, if the "wavy" shape of the main asteroid belt's overall size–frequency distribution (which tends toward a shallower slope near $D \sim 1$ km) noted by Bottke et al. (2005) applies to the Themis family, our simple power-law extrapolation of the observed size distribution of asteroids in the near-MMR region may overestimate the number of $D \geqslant 1$ km Themis family asteroids by a factor of a few. That said, Bottke et al. (2005) also specifically model a "Themis-style" catastrophic fragmentation event and find a size–frequency distribution that is relatively well characterized by a single power law over the range of sizes ($D \sim 1$ km to $D \sim 20$ km) that is relevant to our analysis. It is also possible that some nuclei of observably active comets could be smaller than $D = 1$ km. Pushing to smaller sizes would increase the size of the relevant source population in the Themis family, which would then proportionally increase the expected number of relevant objects from the family that escape onto JFC-like orbits.

As discussed earlier, nongravitational forces may increase the expected rate of Themis family objects evolving onto JFC-like orbits compared to the rate computed from purely gravitational integration results by a factor of two or more, while the much higher fraction of Themis family asteroids with dynamical clones relative to just the objects themselves that

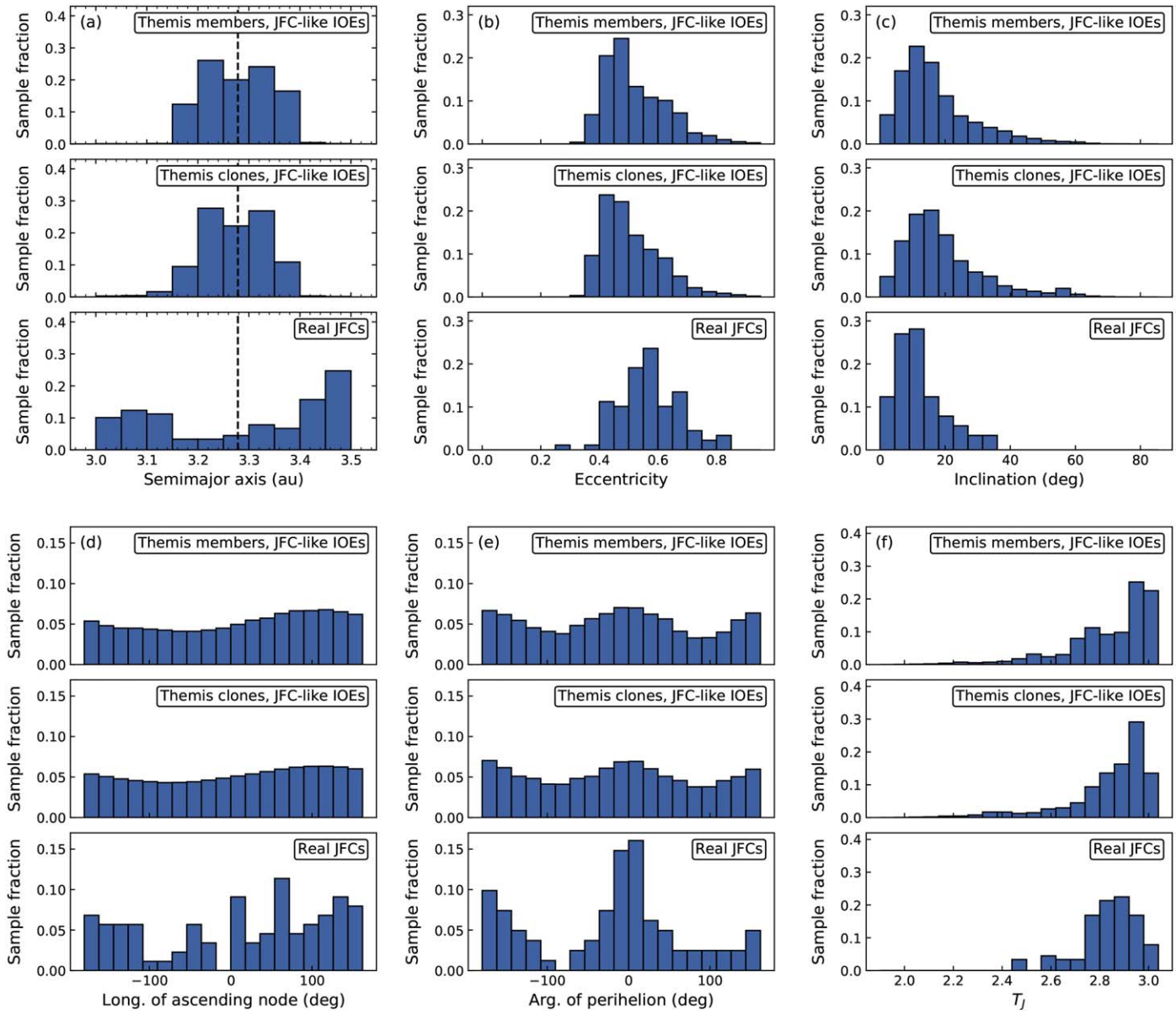

Figure 4. Histograms of the (a) semimajor axes (where the location of the 2:1 MMR is marked with a vertical dashed line in all panels), (b) eccentricities, (c) inclinations, (d) longitudes of the ascending node, (e) arguments of perihelion, and (f) Tisserand parameters with respect to Jupiter of the JFC-like IOEs of real Themis family objects (top panels), the JFC-like IOEs of dynamical clones (middle panels), and current orbits of real JFCs (bottom panels), restricted to only those JFC-like IOEs of test particles and the 89 real JFCs where 3.0 au $< a_{\rm osc} <$ 3.5 au.

evolve onto JFC-like orbits indicates that other perturbations (e.g., collisions) could further increase this flux. Lastly, we see indications that the 100 Myr integration period we use in this work may be too short to capture the full evolution of Themis family objects evolving via resonances other than the 2:1 MMR, potentially causing our analysis to underestimate the full steady-state flux of objects that ultimately reach JFC-like orbits (Section 4.3).

Given all of these complicating factors, our calculation above that ∼20 objects from the Themis family with the potential to mimic active JFCs from the outer solar system should be present at any given time should be considered an order of magnitude estimate only. As such, we conclude that there may be tens of such objects at any given time (compared to a total population of ∼600 known JFCs cataloged by JPL[9] as of 2019 October 1).

4. Discussion

4.1. Possible Dynamical Pathways

Investigation of the evolution of individual particles that reach JFC-like IOEs in our purely gravitational integrations indicate that most of these particles experience eccentricity excitation due to the nearby 2:1 MMR. This excitation in turn lowers their perihelia, causing them to interact more strongly with planets other than Jupiter, with which we find that many test particles experience numerous close encounters during their transition to low-T_J JFC-like orbits. We specifically find

[9] https://ssd.jpl.nasa.gov/?sb_elem

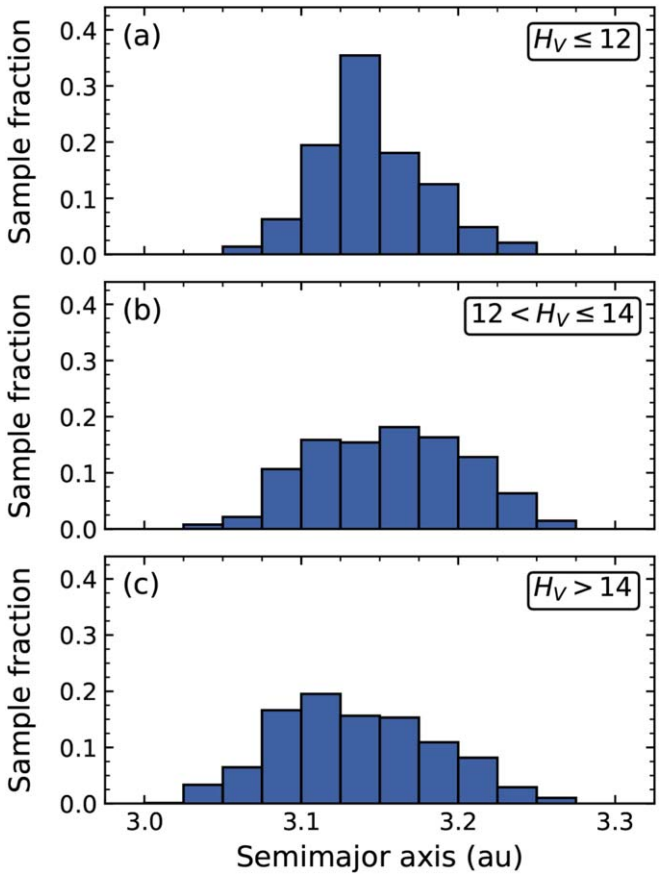

Figure 5. Histograms of semimajor axis distributions of Themis family asteroids in three different absolute magnitude bins—(a) $H_V \leqslant 12$, (b) $12 < H_V \leqslant 14$, and (c) $H_V > 14$—where the population of currently known outer main belt asteroids is believed to be complete for $H_V < 14.4$ (see Granvik et al. 2017), meaning that the distributions in panels (a) and (b) should reflect complete subpopulations.

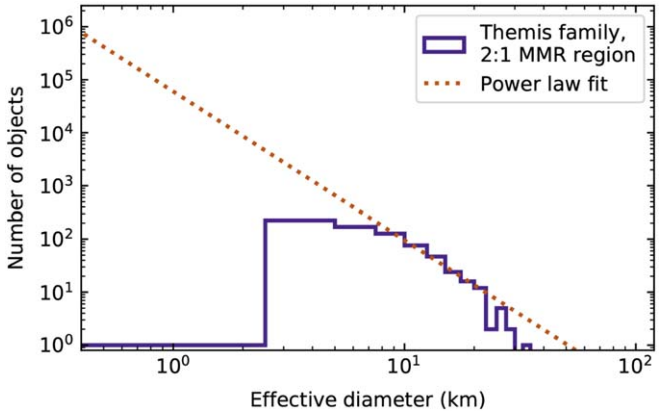

Figure 6. Differential size–frequency distributions of the portion of the Themis family found within the region of influence of the 2:1 MMR defined in Section 3.1 (solid purple line) along with a corresponding power-law fit (dotted orange line).

that 58.8%, 84.6%, 99.7%, and 87.7% of real Themis family asteroids and their dynamical clones with JFC-like IOEs experience close encounters with Venus, Earth, Mars, and Saturn, respectively. These interactions likely play a significant role in driving these particles to comet-like T_J values considering that these other planets represent additional massive perturbers that are not accounted for in the idealized three-body system (i.e., the Sun, Jupiter, and the small body in question) on which the T_J approximation is based.

In our first set of follow-up integrations which included the Yarkovsky effect but no terrestrial planets, encounters with Venus, Earth, and Mars of course did not occur, but evolution onto low-T_J JFC-like orbits by Themis family asteroids still did. This suggests that the observed evolution of particles toward comet-like T_J values can also be driven by a combination of the Yarkovsky effect and interactions with Saturn alone as an additional planetary perturber, even for objects that do not have close encounters with the terrestrial planets.

4.2. Implications for Currently Known JFCs

If Themis family objects are present on JFC-like orbits in appreciable numbers, the next key question is whether they would be expected to be icy enough to support sublimation like other JFCs. Expected depths-to-ice in thermal models of asteroids depend on factors like the thermal properties of mantle material, obliquity, and latitude, but these depths have the potential to be quite shallow at the polar regions of low-obliquity outer main-belt objects formed in recent catastrophic disruption events (Schörghofer 2008, 2016). Thermal modeling by Schörghofer & Hsieh (2018) indicates that young (e.g., $\lesssim$10 Myr old), icy outer-belt asteroids could still retain polar near-surface ice under certain conditions, and therefore could potentially join the active JFC population for a (currently poorly constrained) period of time.

As of 2019 November 1, there are 23 known active JFCs (Table 2; where three are classified as defunct) with 3.15 au $< a <$ 3.40 au, the semimajor axis range containing most of the JFC-like IOEs we find for Themis family objects in our integrations. For reference, an additional ~500 currently inactive asteroids with dynamically JFC-like orbits within this semimajor axis range are also cataloged by JPL. Notably, 210P/Christensen is the only active JFC among these objects that overlaps with the list of JFCs with potential asteroidal origins identified by Fernández & Sosa (2015). Given that we cannot say how many of the Themis family objects found to evolve onto JFC-like orbits in our integrations will actually become active and for how long from our dynamical results alone (Section 3.2), we emphasize that we cannot currently say whether any known JFCs may actually be from the Themis family or how many active JFCs with Themis family origins that we should expect to find in general at any given time.

Several of the aforementioned JFCs in our semimajor axis range of interest have been previously observationally characterized, such as 16P/Brooks 2 ($a = 3.358$ au; e.g., Sekanina 1997; Kiselev et al. 2002), 43P/Wolf–Harrington ($a = 3.350$ au; e.g., Snodgrass et al. 2006; Fink 2009, and references within), 104P/Kowal 2 ($a = 3.263$ au; e.g., Snodgrass et al. 2006), and 124P/Mrkos ($a = 3.309$ au; e.g., Licandro et al. 2003), but many others have not been studied in much detail or at all. Interestingly, 16P/Brooks 2 and 43P/Wolf–Harrington have both been found to be depleted in carbon-chain species (i.e., C_2 and C_3; Schleicher et al. 1993; A'Hearn et al. 1995; Cochran et al. 2012). Whether such depletion points to possible asteroidal origins is unclear (these two objects are certainly not the only carbon chain depleted comets to be identified), but could warrant further investigation. Meanwhile, the nucleus of 124P/Mrkos has been found to be spectroscopically similar to D-type asteroids

Table 2
JFCs with 3.15 au $< a <$ 3.40 au

Comet	a[a]	e[b]	i[c]	q[d]	Q[e]	T_J[f]
16P/Brooks 2	3.358	0.563	4.26	1.4667	5.250	2.873
43P/Wolf–Harrington	3.350	0.595	15.97	1.3570	5.343	2.793
83D/Russell 1	3.338	0.517	22.66	1.6115	5.064	2.824
104P/Kowal 2	3.263	0.639	10.25	1.1791	5.347	2.794
124P/Mrkos	3.309	0.506	31.72	1.6348	4.984	2.742
210P/Christensen	3.193	0.829	10.18	0.5445	5.842	2.491
213P/Van Ness	3.347	0.407	10.38	1.9833	4.711	2.995
218P/LINEAR	3.342	0.491	18.17	1.7011	4.983	2.884
224P/LINEAR-NEAT	3.342	0.437	14.73	1.8818	4.803	2.951
267P/LONEOS	3.290	0.593	5.37	1.3377	5.242	2.856
294P/LINEAR	3.200	0.595	19.09	1.2977	5.103	2.818
304P/Ory	3.243	0.574	2.76	1.3822	5.104	2.896
337P/*WISE*	3.291	0.498	15.40	1.6530	4.929	2.911
365P/PANSTARRS	3.186	0.573	9.84	1.3591	5.012	2.897
D/1770 L1 (Lexell)	3.153	0.786	1.55	0.6744	5.632	2.612
D/1978 R1 (Haneda-Campos)	3.290	0.665	5.95	1.1014	5.479	2.762
P/2000 R2 (LINEAR)	3.338	0.584	3.22	1.3899	5.287	2.857
P/2008 WZ96 (LINEAR)	3.357	0.510	6.96	1.6462	5.067	2.922
P/2013 T2 (Schwartz)	3.393	0.528	9.35	1.5996	5.185	2.886
P/2013 YG46 (Spacewatch)	3.305	0.454	8.11	1.8044	4.806	2.980
P/2015 J3 (NEOWISE)	3.350	0.554	8.13	1.4940	5.207	2.876
P/2016 P1 (PANSTARRS)	3.230	0.294	25.77	2.2805	4.179	2.967
P/2019 A8 (PANSTARRS)	3.354	0.439	2.97	1.8828	4.826	2.992

Notes.
[a] Semimajor axis, in au.
[b] Eccentricity.
[c] Inclination, in degrees.
[d] Perihelion distance, in au.
[e] Aphelion distance, in au.
[f] Tisserand parameter value with respect to Jupiter.
[g] References: [1] (A'Hearn et al. 1995).

(Licandro et al. 2003), which is consistent with spectra obtained for nuclei of other JFCs (e.g., Lamy et al. 2004), but not of Themis family asteroids (see Hsieh et al. 2018). Further systematic physical and compositional characterization of comets with semimajor axes in the range where we expect most of the Themis family objects that evolve onto JFC-like orbits to be found will be very important for assessing whether physical evidence supports our conclusion that Themis family objects may be present in the active JFC population.

4.3. Expected Asteroidal Contribution to the JFC Population

Some theoretical analyses have found that assumed source populations in the outer solar system (primarily, the scattered disk) do not produce a sufficient number of JFCs to supply the observed population (e.g., Volk & Malhotra 2008; Nesvorný et al. 2017), suggesting that various model assumptions could require modification, or that other sources may also contribute to the population. In fact, other studies have shown that JFCs could potentially also originate in the Jovian (or even Neptunian) Trojan and Hilda populations (e.g., Levison et al. 1997; Di Sisto et al. 2005, 2019; Horner & Lykawka 2010). Asteroids throughout the main belt are well-known to be driven by MMRs and secular resonances into occasionally escaping from the main-belt and evolving onto NEO orbits (e.g., Bottke et al. 2002; Greenstreet et al. 2012; Michtchenko et al. 2016; Granvik et al. 2017, 2018). Some of these objects may even reach cometary orbits, though this appears to have generally not been explicitly considered in studies to date investigating NEO origins.

The results presented here make it tempting to speculate that the Themis family could be one of the additional sources needed to supply the observed population of JFCs. However, the narrow semimajor axis range near the 2:1 MMR (which is much narrower than the range over which most JFCs are found; Figure 4), within which we find most JFC-like objects produced by the Themis family, suggests that the family is, at best, a minor contributor. That said, this work focuses on current Themis family members, rather than the entire outer asteroid belt, much of which could be intrinsically icy and could also include Themis family members that have escaped the family in the past but currently persist on main-belt orbits.

An additional nuance is that we see indications that a 100 Myr integration period may not be long enough to capture the full steady-state flux of all Themis family asteroids onto JFC-like orbits. In particular, the evolution of particles evolving to JFC-like orbits via resonances other than the 2:1 MMR may not be fully captured by the integrations presented here, which could affect the total number and semimajor axis distribution of JFC-like objects found to be produced by the family. We recall that a typical pathway followed by a Themis family asteroid that evolves onto a JFC-like orbit involves (1) some initial amount of time spent within the Themis family, (2) eccentricity and inclination excitation due to a nearby MMR, during which the object exits the Themis family but is still confined to the main belt, and (3) eventual evolution onto a JFC-like orbit (Section 4.1). In our integrations, the median time spent in the second stage of this evolution by test particles that eventually reach JFC-like orbits is 5.1 Myr for particles evolving via the 2:1 MMR, and 42.0 Myr for particles evolving via the 9:4 or 11:5 MMRs. The substantial fraction of our total integration period represented by the latter timescale suggests that there may be many particles that will eventually reach JFC-like orbits that are still in this second stage of their evolution at the end of our integrations (e.g., particles that first reach non-Themis MBA-like orbits relatively late in our integrations or that spend longer than the median amount of time in this stage of their evolution). A complete accounting of the steady-state flux of Themis family asteroids to JFC-like orbits should include the eventual contribution of these objects. A follow-up study using a longer integration period that better accounts for the slower dynamical evolution of objects driven by relatively weak resonances would be very useful for ascertaining both the true steady-state flux and orbital element distribution of Themis family asteroids evolving onto JFC-like orbits.

4.4. Other Future Work

Larger-scale dynamical studies that sample the entire outer asteroid belt and use longer integration periods, while also including nongravitational forces and the terrestrial planets as

perturbers, are likely needed to assess the asteroid belt's true contribution to the population of dynamically JFC-like small solar system bodies that could potentially comprise part of the active JFC population if they also happen to be sufficiently icy. Evolution of main-belt objects onto JFC-like orbits may very well have occurred in previous dynamical studies investigating NEO origins, but simply not been noticed due to the evolution of T_J values not being explicitly considered in those studies. Therefore, while new large-scale and longer-term dynamical integrations to follow up the work presented here would be highly desirable, one simple next step could be to reexamine integration data sets generated by large-scale NEO population studies to identify asteroids that evolve onto low-T_J orbits.

Meanwhile, theoretical modeling of the thermal evolution of objects evolving from the asteroid belt to JFC-like orbits would be useful for improving predictions about how many such objects could retain enough near-surface ice to support observable sublimation-driven activity. Thermal modeling aimed at placing constraints on the active lifetimes of these objects would also be useful for estimating the total number of objects from the Themis family on JFC-like orbits that could actually be active at any given time.

5. Summary

In this work, we present the results of numerical integrations of test particles representing members of the Themis asteroid family aimed at investigating dynamical pathways from potentially icy Themis family asteroids and the active Jupiter-family comet population. We report the following key results:

1. Purely gravitational numerical integrations show that on the order of a few percent of current Themis family asteroids escape the family every 100 Myr and evolve onto orbits that are dynamically similar to those of JFCs. If ice is widespread on Themis family objects as some independent studies have suggested and can be preserved in near-surface layers until those objects evolve onto JFC-like orbits, these dynamical results suggest that these objects have the potential to become active and thus mimic JFCs from the outer solar system despite originating in the main asteroid belt.
2. The dynamical pathway by which most Themis family asteroids reach JFC-like orbits in our integrations is one in which objects near the 2:1 mean-motion resonance with Jupiter have their eccentricities and inclinations excited by the resonance, which then causes their orbits to approach and cross those of the major planets, particularly the terrestrial planets, Jupiter, and Saturn. Many of these objects subsequently experience close encounters with these planets, which appear to help to drive their Tisserand parameter values with respect to Jupiter from asteroid-like values ($T_J > 3$) down to JFC-like values ($2 < T_J < 3$).
3. We estimate that, at any given time, there may be tens of objects from the Themis family on JFC-like orbits with the potential to mimic active JFCs from the outer solar system (compared to a total population of ~600 currently known JFCs), although not all, or even any, may necessarily be observably active. Calculations based on our purely gravitational integration results indicate that ~20 objects with $D \geqslant 1$ km from the Themis family may be on JFC-like orbits at any given time, but given uncertainties in the size of the relevant source population in the Themis family and the precise effects of factors like nongravitational forces and collisional perturbations, we regard this simply as an order of magnitude estimate of the number of dynamically evolved Themis family objects with the potential to mimic active JFCS.
4. Dynamically evolved Themis family asteroids that reach JFC-like orbits have orbital element distributions while on such orbits that are largely compatible with those of real JFCs, indicating that they could plausibly infiltrate the JFC population without being obvious dynamical outliers. One distinguishing feature that could help to identify these objects is that they have semimajor axes within 0.125 au from the 2:1 mean-motion resonance with Jupiter (i.e., between 3.15 au and 3.40 au) for the vast majority (~90%) of their time on such orbits, consistent with the strong role that this resonance plays in their dynamical evolution. That said, we find indications that longer integrations could change both the predicted abundance and orbital element distribution of dynamically evolved Themis family asteroids on JFC-like orbits.

Integration data are available upon request by contacting the corresponding author.

We thank an anonymous reviewer for helpful comments that improved this paper. H.H.H., K.W., and N.S. acknowledge support from NASA via the Solar System Workings program (Grant 80NSSC17K0723) as well as Solar System Exploration Research Virtual Institute (SSERVI) Cooperative Agreement grant NNH16ZDA001N. B.N. acknowledges support by the Ministry of Education, Science and Technological Development of the Republic of Serbia, Project 176011. The authors acknowledge the PSI Computing Center (PSICC) for providing HPC resources that contributed to the research results reported here.

Software: `matplotlib` (Hunter 2007), `mercury` (Chambers 1999), `orbfit` and `ORBIT9` (Milani & Nobili 1988, http://adams.dm.unipi.it/orbfit/).

ORCID iDs

Henry H. Hsieh https://orcid.org/0000-0001-7225-9271
Bojan Novaković https://orcid.org/0000-0001-6349-6881
Kevin J. Walsh https://orcid.org/0000-0002-0906-1761
Norbert Schörghofer https://orcid.org/0000-0002-5821-4066

References

A'Hearn, M. F., Millis, R. C., Schleicher, D. O., Osip, D. J., & Birch, P. V. 1995, Icar, 118, 223
Bottke, W. F., Durda, D. D., Nesvorný, D., et al. 2005, Icar, 175, 111
Bottke, W. F., Morbidelli, A., Jedicke, R., et al. 2002, Icar, 156, 399
Bottke, W. F., Jr., Vokrouhlický, D., Rubincam, D. P., & Nesvorný, D. 2006, AREPS, 34, 157
Campins, H., Hargrove, K., Pinilla-Alonso, N., et al. 2010, Natur, 464, 1320
Chambers, J. E. 1999, MNRAS, 304, 793
Cochran, A. L., Barker, E. S., & Gray, C. L. 2012, Icar, 218, 144
Di Sisto, R. P., Brunini, A., Dirani, L. D., & Orellana, R. B. 2005, Icar, 174, 81
Di Sisto, R. P., Ramos, X. S., & Gallardo, T. 2019, Icar, 319, 828
Fernández, J. A., & Sosa, A. 2015, P&SS, 118, 14
Fernández, Y. R., Kelley, M. S., Lamy, P. L., et al. 2013, Icar, 226, 1138
Fernández, Y. R., Lisse, C. M., Ulrich Käufl, H., et al. 2000, Icar, 147, 145
Fink, U. 2009, Icar, 201, 311
Granvik, M., Morbidelli, A., Jedicke, R., et al. 2018, Icar, 312, 181
Granvik, M., Morbidelli, A., Vokrouhlický, D., et al. 2017, A&A, 598, A52

Greenstreet, S., Ngo, H., & Gladman, B. 2012, Icar, 217, 355
Haghighipour, N. 2009, M&PS, 44, 1863
Hargrove, K. D., Emery, J. P., Campins, H., & Kelley, M. S. P. 2015, Icar, 254, 150
Horner, J., & Lykawka, P. S. 2010, IJAsB, 9, 227
Hsieh, H. H., & Haghighipour, N. 2016, Icar, 277, 19
Hsieh, H. H., & Jewitt, D. 2006, Sci, 312, 561
Hsieh, H. H., Novaković, B., Kim, Y., & Brasser, R. 2018, AJ, 155, 96
Hsieh, H. H., Yang, B., Haghighipour, N., et al. 2012, ApJL, 748, L15
Hunter, J. D. 2007, CSE, 9, 90
Jewitt, D. 1991, ASSL, 167, 19
Kiselev, N., Jockers, K., & Rosenbush, V. 2002, EM&P, 90, 167
Kresák, L. 1972, in IAU Symp. 45, The Motion, Evolution of Orbits, and Origin of Comets, ed. G. Aleksandrovich Chebotarev, E. I. Kazimirchak-Polonskaia, & B. G. Marsden (Dordrecht: Reidel), 503
Lamy, P. L., Toth, I., Fernandez, Y. R., & Weaver, H. A. 2004, in Comets II, ed. M. C. Festou, H. U. Keller, & H. A. Weaver (Tucson, AZ: Univ. Arizona Press), 223
Levison, H. F., Shoemaker, E. M., & Shoemaker, C. S. 1997, Natur, 385, 42
Licandro, J., Campins, H., Hergenrother, C., & Lara, L. M. 2003, A&A, 398, L45
Masiero, J. R., DeMeo, F. E., Kasuga, T., & Parker, A. H. 2015, in Asteroids IV, ed. P. Michel, F. E. DeMeo, & W. F. Bottke (Tucson, AZ: Univ. Arizona Press), 323
Michtchenko, T. A., Lazzaro, D., & Carvano, J. M. 2016, A&A, 588, A11
Milani, A., & Nobili, A. M. 1988, CeMec, 43, 1
Morbidelli, A., Zappala, V., Moons, M., Cellino, A., & Gonczi, R. 1995, Icar, 118, 132
Murray, C. D., & Dermott, S. F. 2000, Solar System Dynamics (Cambridge: Cambridge Univ. Press)
Nesvorny, D. 2015, Nesvorny HCM Asteroid Families, NASA Planetary Data System, EAR-A-VARGBDET-5-NESVORNYFAM-V3.0PDSShttps://pds.nasa.gov/ds-view/pds/viewProfile.jsp?dsid=EAR-A-VARGBDET-5-NESVORNYFAM-V3.0
Nesvorný, D., Vokrouhlický, D., Dones, L., et al. 2017, ApJ, 845, 27
Rivkin, A. S., & Emery, J. P. 2010, Natur, 464, 1322
Schleicher, D. G., Bus, S. J., & Osip, D. J. 1993, Icar, 104, 157
Schörghofer, N. 2008, ApJ, 682, 697
Schörghofer, N. 2016, Icar, 276, 88
Schörghofer, N., & Hsieh, H. H. 2018, JGRE, 123, 2322
Sekanina, Z. 1997, A&A, 318, L5
Snodgrass, C., Lowry, S. C., & Fitzsimmons, A. 2006, MNRAS, 373, 1590
Spoto, F., Milani, A., & Knežević, Z. 2015, Icar, 257, 275
Tancredi, G. 2014, Icar, 234, 66
Vokrouhlický, D., Brož, M., Bottke, W. F., Nesvorný, D., & Morbidelli, A. 2006, Icar, 182, 118
Volk, K., & Malhotra, R. 2008, ApJ, 687, 714
Walsh, K. J., Delbó, M., Bottke, W. F., Vokrouhlický, D., & Lauretta, D. S. 2013, Icar, 225, 283
Wang, X., & Malhotra, R. 2017, AJ, 154, 20